Associations between serum concentrations of perfluoroalkyl substances and DNA methylation in women exposed through drinking water: A pilot study in Ronneby, Sweden

Yiyi Xu [a], Simona Jurkovic-Mlakar [b], Christian H. Lindh [c], Kristin Scott [c], Tony Fletcher [d], Kristina Jakobsson [a,e], Karin Engström [f,*]

[a] School of Public Health and Community Medicine, Institute of Medicine, University of Gothenburg, Gothenburg, Sweden
[b] CANSEARCH Research Laboratory, Faculty of Medicine, University of Geneva, Geneva, Switzerland
[c] Occupational and Environmental Medicine, Department of Laboratory Medicine, Lund University, Lund, Sweden
[d] London School of Hygiene and Tropical Medicine, London, United Kingdom
[e] Occupational and Environmental Medicine, Sahlgrenska University Hospital, Gothenburg, Sweden
[f] EPI@LUND, Department of Laboratory Medicine, Lund University, Lund, Sweden

ARTICLE INFO

ABSTRACT

Background: Perfluoroalkyl substances (PFAS) are widespread synthetic substances with various adverse health effects. A potential mechanism of toxicity for PFAS is via epigenetic changes, such as DNA methylation. However, few studies have evaluated associations between PFAS exposure and DNA methylation among adults, and data is especially scarce for women. Furthermore, exposure to environmental pollutants has been associated with epigenetic age acceleration, but no studies have yet evaluated whether PFAS is associated with epigenetic age acceleration.
Objectives: To investigate whether exposure to PFAS is associated with alteration of DNA methylation and epigenetic age acceleration among women.
Methods: In this observational pilot study, 59 women (aged 20–47 years at enrollment in 2014) from Ronneby, Sweden, an area with historically high PFAS exposure due to local drinking water contamination, were divided into three PFAS exposure groups (low, medium, and high). Genome-wide methylation of whole-blood DNA was analyzed using the Infinium MethylationEPIC BeadChip. Ingenuity Pathway Analysis was used for *in silico* functional assessment. Epigenetic age acceleration was derived from the DNA methylation data using Horvath's epigenetic skin and blood clock.
Results: 117 differentially methylated positions ($q < 0.017$) and one near-significantly differentially methylated region (*S100A13*, FWER = 0.020) were identified. *In silico* functional analyses suggested that genes with altered DNA methylation ($q < 0.05$) were annotated to cancer, endocrine system disorders, reproductive system disease, as well as pathways such as estrogen receptor signaling, cardiac hypertrophy signaling, PPARα/RXRα activation and telomerase signaling. No differences in epigenetic age acceleration between PFAS exposure groups were noted ($p = 0.43$).
Conclusion: The data suggests that PFAS exposure alters DNA methylation in women highly exposed to PFAS from drinking water. The observed associations should be verified in larger cohorts, and it should also be further investigated whether these changes in methylation also underlie potential phenotypic changes and/or adverse health effects of PFAS.

1. Introduction

Perfluoroalkyl substances (PFAS) are a group of man-made persistent organic pollutants (POPs). Drinking water contaminated by PFAS affects the general population worldwide (Banzhaf et al. 2017; Guelfo and Adamson 2018; Willach et al. 2016). Many countries have announced national action guidelines or regulations for PFAS levels in drinking water (Wilhelm et al. 2008, Drinking water inspectorate 2009, Livsmedelsverket, 2016). However, PFAS already present in the environment are still potentially harmful because of environmental persistence, bioaccumulation and long half-life in human (EFSA 2020).

Perfluorooctane sulfonic acid (PFOS) and perfluorooctanoic acid (PFOA) are two of the most widely studied PFAS. Several studies have linked PFOS and PFOA exposure to various adverse health effects, such as immunotoxicity, endocrine disrupting effects and metabolic effects (EFSA 2018). Recently, studies about perfluorohexane sulfonic acid (PFHxS) have emerged, since it is found in soil, water and a variety of biota in the vicinity of firefighting training areas following the historical use of aqueous film forming foam concentrate (AFFF) firefighting foam. Studies have shown similar effects of PFOA, PFOS and PFHxS on human health (EFSA 2020), however, the exact modes of PFAS toxicity are still not clear. Epigenetic changes, such as DNA methylation, have been proposed as a possible molecular mechanism underlying adverse health effects of pollutants (Baccarelli and Bollati. 2009). DNA methylation occurs predominantly on cytosines (C) that are followed by guanine (G) residues, referred to as CpG sites. By influencing the gene transcription, DNA methylation often precedes the development of measurable subclinical effects or pathologies (Maunakea et al. 2010) and can therefore serve as a sensitive effect biomarker of environmental pollutants.

The association between DNA methylation and aging is well established (Johansson et al. 2013, Florath et al. 2014). Data from whole-genome DNA methylation arrays can be used to estimate the so-called epigenetic age across a broad spectrum of human tissues and cell types using an "epigenetic clock" based on a number of age-dependent CpG signatures (Horvath 2013; Horvath et al. 2018). Accelerated epigenetic aging, i.e., a discrepancy between the biological and chronological age, measured in DNA from whole blood, correlates with increased mortality (Marioni et al. 2015a), and impaired physical and cognitive function (Marioni et al. 2015b). Additionally, previous studies have seen associations between POP exposure and epigenetic age acceleration in DNA from whole blood (Curtis et al. 2019; Lind et al. 2018). Thus, epigenetic age acceleration could also be a mechanism underlying adverse health effects of environmental pollutants. However, to the best of our knowledge, the effect of PFAS on epigenetic age acceleration has not yet been investigated.

Epidemiological studies regarding associations between PFOS and/or PFOA exposure, and changes in DNA methylation patterns have comprised newborns from mother–child cohorts. These studies revealed associations of exposure with decreased global DNA methylation in the cord blood or umbilical cord serum (Guerrero-Preston et al. 2010; Liu et al., 2018a, 2018b), and with methylation changes in specific DNA methylation sites or regions in gene-specific whole genome analyses in cord blood (Kingsley et al. 2017; Leung et al. 2018; Miura et al. 2018). Few studies have evaluated associations between PFOS and/or PFOA exposure and changes in DNA methylation patterns among adults. One study evaluated LINE-1 methylation (a surrogate marker for global DNA methylation) in peripheral blood leukocytes among adults (Watkins et al. 2014) and found exposure to PFOS, but not PFOA, to be associated with increased LINE-1 methylation (no sex-stratified analyses were performed). One study, comprising men only, evaluated genome-wide DNA methylation in leukocytes upon PFAS exposure (van den Dungen et al. 2017). This study revealed associations between PFAS and specific DNA methylation regions, related to genes involved in e.g. carcinogenesis and the immune system. However, no study, to date, has evaluated genome-wide DNA methylation upon PFAS exposure in women. This is of importance, given that DNA methylation can be sex-specific

(McCarthy et al. 2014) and age-specific (Day et al. 2013, Sikdar et al. 2019) and that epidemiological studies have showed sex-specific associations between PFAS and earlier menopause and lower estradiol levels (Knox et al. 2011), as well as higher thyroid hormones in adult women (Wen et al. 2013, Blake et al. 2018). Thus, further knowledge of how PFAS exposure is associated to DNA methylation in women's blood is needed.

In the current pilot study, we aimed to investigate whether PFAS exposure (measured in serum) is associated with alteration of DNA methylation in whole blood and epigenetic age acceleration, two potential mechanisms of PFAS toxicity, in women. Furthermore, we performed *in silico* analyses to identify potential biological functions associated with genes with altered DNA methylation.

2. Materials and methods

2.1. Study participants

The study participants were a subset of the Ronneby Biomarker Cohort and its reference group from Karlshamn (Li et al. 2018). The Ronneby Biomarker Cohort comprises 3297 individuals from Ronneby, Sweden, where a third of households have been exposed to highly PFAS-contaminated drinking water from the mid-1980s until December 2013. Biomonitoring performed in June 2014, shortly after cessation of exposure, revealed very high serum levels of PFAS, which were dominated by PFOS, PFHxS, and to a lesser extent, PFOA, in individuals living in the area with contaminated drinking water in Ronneby. The reference group was recruited in 2016 and comprises 226 individuals from Karlshamn, a nearby municipality with uncontaminated municipal drinking water supply and with similar socioeconomic status. Serum levels of PFAS in the reference group were very low and comparable with those of the Swedish general population (Li et al. 2018).

The subset included in this study are 64 non-smoking and non-pregnant women aged 20–47 years at recruitment. These 64 women included all 53 women that were included in our previous study evaluating the association between PFAS exposure and microRNA expression in serum (Xu et al. 2020). The blood samples used for PFAS and DNA methylation analysis were taken in September 2017 for Ronneby participants, and in May 2016 for Karlshamn reference group, respectively. The grouping of individuals into exposure groups were conducted in the same way as described by Xu et al. (2020). Briefly, the selection of individuals to be included in this study was based on their serum PFOS concentrations (measured prior to the selection of participants, Section 2.2), allowing the division of participants into three exposure groups (low, medium and high exposure group, Table 1). Serum PFOS levels were used as a proxy for PFHxS, PFOA and sum of three PFAS because of the high correlation between each other (Spearman's $r > 0.8$, $p < 0.001$

Table 1

Descriptive statistics [median (range)] for the study participants consisting of 59 non-smoking and non-pregnant women.

PFAS exposure group	Low (n = 21)	Medium (n = 20)	High (n = 18)	*p*-value[a]
Age (years)	36 (26–45)	37 (21–45)	39 (21–47)	0.95
BMI (kg/m^2)	24 (20–31)	23 (18–30)	24 (19–37)	0.30
PFOS (ng/ml)	3 (0–11)	56 (16–112)	230 (113–380)	<0.001
PFHxS (ng/ml)	1 (0–9)	43 (11–136)	200 (96–371)	<0.001
PFOA (ng/ml)	2 (0–4)	2 (1–9)	10 (4–24)	<0.001
Sum of three PFAS (ng/ml)	6 (2–22)	100 (30–257)	438 (217–739)	<0.001

Abbreviations: BMI, body mass index; PFHxS, perfluorohexane sulfonic acid; PFOS, perfluorooctane sulfonic acid; PFOA, perfluorooctanoic acid; PFAS, perfluoroalkyl substances.

[a] P-values from Kruskal-Wallis test in between-group comparisons for PFAS exposure group.

for all pairs). Additionally, the descriptive analysis of serum levels of PFOS, PFHxS, PFOA and sum of three PFAS confirmed our assumption of different levels of exposure in the three groups (Table 1).

The low exposure group included 22 women from the reference group (PFOS range 0–11 ng/ml). The other 42 women from Ronneby Biomarker Cohort were grouped into medium (PFOS range 16–112 ng/ml) and high (PFOS range 113–380 ng/ml) exposure groups. The mean age and body mass index (BMI) in the exposure groups were similar ($p > 0.05$ in between-group comparisons, Kruskal-Wallis test). Five subjects were excluded because of failure of the DNA methylation analysis (no data acquired from the DNA methylation array). Therefore, 59 women were included as participants in the study.

All participants gave informed written consent. The study was approved by the Regional Ethical Review Board in Lund, Sweden (approved on date 22 April 2014; approval number 2014/4).

2.2. Serum PFAS concentration analysis

Venous blood samples were collected in 5-ml Becton Dickinson (Plymouth, UK) vacutainer tubes without gel. The serum was transferred to cryotubes and stored at –80 °C at a biobank in Lund (Sweden), and total non-isomer–specific PFHxS, PFOS, and PFOA levels were analyzed at the Department of Occupational and Environmental Medicine in Lund (Sweden). Serum PFAS concentrations were analyzed as described by Li et al. (2018). Briefly, after thawing and vortexing samples, the proteins were precipitated using acetonitrile by vigorous shaking for 30 min. The aliquots of 25 μL serum were added together with 75 μL of water and isotopically labeled internal standards for all compounds. The samples were then centrifuged, and 1 μL of the supernatant was analyzed using liquid chromatography (LC) (UFLCXR, SHIMADZU Corporation, Kyoto, Japan) connected to tandem mass spectrometry (MS/MS) (QTRAP 5500, AB Sciex, Foster City, CA, USA). In all batches, chemical blanks and three quality control (QC) samples, prepared in-house from serum spiked with different PFAS were included. Coefficients of variation of QC samples at 100 ng/mL were 6% for PFHxS and PFOS and 8% for PFOA. The limits of detection were 0.5 ng/mL for PFHxS and PFOS and 0.4 ng/mL for PFOA.

2.3. DNA methylation analysis

The blood samples used for DNA methylation analysis were taken at the same time as the samples for PFAS analysis. DNA was extracted from the whole blood using Chemagic Maxiprep, (PerkinElmer, Rodgau, Germany). DNA quality was evaluated using a NanoDrop spectrophotometer (NanoDrop Products, Wilmington, DE), based on the 260 nm/280 nm ratio (all samples had a ratio ~ 1.8 which is generally accepted as "pure" for DNA). Next, 500 μg DNA was bisulfite-treated using the EZ DNA Methylation kit (Zymo Research, Irvine, CA). DNA samples were randomized for distribution in a 96-well analysis plate. The entire bisulfite-treated DNA samples were used for the DNA methylation analysis. Genome-wide DNA methylation was determined at the Center for Translational Genomics (CTG), Lund University, Sweden, using the Infinium MethylationEPIC BeadChip (lllumina, San Diego, CA) for the analysis of approximately 850,000 specific markers of DNA methylation in the genome. All beadchips were from the same batch. Image processing, background correction, quality control, filtering, and normalization using the quantile normalization procedure were performed using the R package minfi (Fortin et al. 2017). Five samples failed the analyses for unknown reasons and data for the corresponding participants was excluded. The other (59) samples performed well (the detection *p*-value was below 0.01 for at least > 98% of CpGs). CpGs for which the detection *p*-value was above 0.01 in >20% of samples were removed. Probes with common single-nucleotide polymorphisms (according to the function dropLociWithSnps in minfi) and probes in the Y chromosome were removed. Overall, 831,681 probes were retained and analyzed. DNA methylation data were used to determine the proportion of different cell types (B cells, CD4$^+$ T cells, CD8$^+$ T cells, granulocytes, monocytes, and natural killer cells) from reference datasets for sorted samples using the function estimateCellCounts in minfi (Fortin et al. 2017), as described by Houseman et al. (2012). These proportions were later evaluated as potential covariates in the statistical models (Section 2.5).

2.4. Epigenetic age acceleration analysis

The epigenetic age was estimated using the epigenetic "skin and blood clock" based on 391 CpGs (Horvath et al. 2018). By regressing the estimated epigenetic age to the chronological age, the residual gives each person a value for the epigenetic age acceleration. A positive value of age acceleration indicates that the tissue ages faster than expected, i.e., indicates an accelerating epigenetic clock.

2.5. Statistical analysis

Principal component analysis (PCA) was performed to identify the technical and biological variables that influenced DNA methylation, which then was considered as covariates in linear models. The variables included in the PCA were age, BMI, use of antibiotics, slide (i.e., physical position in the analysis plate) and fractions of estimated cell counts (B cells, CD4$^+$ T cells, CD8$^+$ T cells, granulocytes, monocytes, and natural killer cells). The universally applicable singular value decomposition was employed for PCA. The PCA was used on DNA methylation values expressed as normalized *M* values. Univariate linear regression model analysis was then performed to determine the associations between the principal components, and technical and biological variables using the R package Swamp (Lauss et al. 2013, data not shown). Variables that were significantly associated ($p < 0.05$) with any of the first four principal components were adjusted for in the linear regression models described below. These variables were the technical variable "slide" and the estimated fractions of CD4$^+$ T cells, CD8$^+$ T cells, and neutrophils. Since the determined neutrophil fractions were strongly correlated with CD4$^+$ T cells and CD8$^+$ T cells ($r_s > 0.6$, $p < 0.001$), the model was only adjusted for slide, CD4$^+$ T cells, and CD8$^+$ T cells.

Differentially methylated positions (DMPs) were evaluated by fitting a robust linear regression model to each CpG using the R package limma with adjustments as described above. Pair-wise comparisons between the three exposure groups were performed using a contrast matrix. The group with the lowest exposure was used as reference in all pair-wise comparisons. Empirical Bayes smoothing was applied to the standard errors. Further, *p*-values were adjusted for multiple comparisons for all CpGs by the Benjamini–Hochberg false discovery rate (FDR) method to obtain *q*-values. Additionally, Bonferroni correction was performed for three time's pair-wise group comparisons, therefore a *q*-value of $0.050/3 = 0.017$ or lower was considered statistically significant. To test linear associations, a test of trend was done by performing a model where the exposure group was employed as a continuous variable. *P*-values were adjusted for multiple comparisons for all CpGs by the Benjamini–Hochberg FDR method to obtain *q*-values. A *q*-value of 0.05 or lower was considered statistically significant in the trend test.

Differentially methylated regions (DMRs) were evaluated using the bumphunter function in the R package minfi (Fortin et al. 2017), employing Beta-values. DMRs at least two CpGs long were included. Family-wise error rate (FWER), as implemented in the bumphunter function in minfi, was employed. FWER denotes the probability of making one or more false discoveries, or type I errors during multiple-hypothesis testing. A FWER-value of 0.017 or lower was considered statistically significant (since Bonferroni correction was performed for three time's pair-wise group comparisons).

The correlation between epigenetic age and chronological age were evaluated using Spearman correlation. The differences in epigenetic age acceleration between PFAS exposure groups were analyzed using one-way analysis of variance (ANOVA) with least significant difference

post hoc test using IBM SPSS (Version 25.0; IBM SPSS Statistics for Windows, NY). A *p*-value of 0.05 or lower was considered statistically significant.

2.6. In silico functional analysis

The software Ingenuity Pathway Analysis (IPA) (Ingenuity systems, Redwood City, CA) accesses large databases with detailed and structured findings derived from thousands of biological, chemical, and medical studies (Thomas and Bonchev 2010). Lists of CpGs based on $q <$ 0.05 in the pair-wise comparisons and directions of their associations were uploaded into IPA. For the enrichment analyses, we did not use the more stringent criterion of employing *q*-values of 0.017 or lower, which was employed in the DMP analyses (Section 2.5) due to a too low number of DMPs included. However, we performed additional enrichment analyses with a cut-off of $q < 0.017$ as a sensitivity analysis in addition to the main analyses with a cut-off of $q < 0.05$. The *q*-value cut-off of 0.017 obtained a too low number of genes that were potentially involved in certain canonical pathways, and thus no sufficient confident activity predictions across datasets (z-score) in IPA knowledge base could be calculated and the canonical pathways showed high p-values. Therefore, a criterion of $q < 0.05$ for being considered a DMP in the *in silico* analyses was used instead, in order to be able to conduct a wider analysis for canonical pathways, with more functional directions of the canonical pathways, thus strengthening our *in silico* analyses.

DMPs with known gene symbols were mapped to the corresponding gene objects in the Ingenuity knowledge human database and analyzed for "canonical pathways" and "diseases and biological functions" (analyzed on 08252020). DMPs for all group comparisons together were analyzed as well as DMPs from each group comparison separately. Top pathways were identified by canonical pathway analysis based on two parameters: (1) ratio of the number of genes in the input list mapped to the pathway to the total number of genes mapped to the canonical pathway (from the IPA library of canonical pathways); and (2) *p*-value calculated using the Fisher's exact test and determining the probability that the number of genes in the dataset and canonical pathway was consistent with the null hypothesis of no association between our list of genes and a certain canonical pathway. The overall activation or inhibition state of a canonical pathway was predicted based on a z-score algorithm, where a z-score ≥ 1 indicates increased activation and z-score ≤ 1 indicates decreased activation. For disease and biological function analysis, the *p*-value was calculated using the right-tailed Fisher's exact test.

3. Results

3.1. DMPs in different PFAS exposure group comparisons

We first investigated whether PFAS exposure is associated with differential methylation of specific positions in the genome. We used beadchips to analyze methylation patterns in whole-blood DNA isolated from individuals from low, medium, and high PFAS exposure groups. In the pair-wise comparisons, we identified 96 statistically significant DMPs ($q < 0.017$), comparing high and low exposure group samples; 11 DMPs, comparing high and medium exposure group samples; and 12 DMPs, comparing medium and low exposure group samples. Of these, 117 DMPs were unique. A Venn diagram depicting the number of DMPs per group comparison and overlapping DMPs between group comparisons are shown in Supplemental Fig. S1. We noted that hypomethylation was more common than hypermethylation in the high vs. low exposure group comparison as well as in the trend test (61% of DMPs were hypomethylated for both analyses). No clear hyper or hypomethylation could be seen among DMPs in the other exposure group comparisons, although the number of DMPs were fairly low in those two exposure group comparisons. In the trend test, we identified 248 DMPs with statistically significant trends with increasing exposures ($q < 0.05$), i.e.

constantly hyper- or hypomethylated with increased PFAS exposure.

The statistically significant DMPs in each pair-wise comparison of exposure groups (top 10 DMPs for high vs. low exposure group comparison), as well as the top 10 DMPs in the trend test, are listed in Table 2. All statistically significant DMPs for high vs. low exposure group comparison are shown in Supplemental Table S1. Volcano plots showing the statistical significance (for DMPs with $q < 0.017$) versus magnitude of change (2^logFC) of the DMPs in the different exposure group comparisons are shown in Fig. 1. Three DMPs were statistically significant in more than one exposure group comparison: matrix metallopeptidase 17 gene (*MMP17*), xin actin binding repeat containing 2 (*XIRP2*) and MET proto-oncogene, receptor tyrosine kinase (*MET*). *MMP17* was statistically significant in high vs. low and medium vs. low exposure group comparisons. It showed the same magnitude of negative association with PFAS exposure in both comparisons, i.e. approximately 18% hypomethylation with increased PFAS exposure, and thus *MMP17* did not show a significant trend along with increased PFAS levels (high vs. medium exposure group comparison: 2^logFC = 1.0, $q = 1.0$, trend test $q = 0.18$, Table 2). *XIRP2* was statistically significant in high vs. low exposure and medium vs. low exposure group comparisons and showed approximately 16% hypermethylation with increased PFAS exposure in both group comparisons (Table 2, high vs low exposure group comparison: 2^logFC = 1.16, $q = 0.010$) as well as a significant trend ($q = 0.046$). For *MET,* the directions of associations in different exposure group comparisons were different. Namely, *MET* was hypomethylated when comparing high and medium exposure groups, but hypermethylated when comparing medium and low exposure groups (trend test $q = 1.0$). Additionally, one gene, PHD finger protein 21B gene (*PHF21B*), which was statistically significant in the high vs. low exposure group comparison, also was of borderline significance ($q = 0.026$) in the high vs. medium exposure group comparison, and showed consistent hypomethylation with increasing PFAS exposure (trend test $q = 0.024$).

The results of the trend test showed similar DMPs as the analysis for the high vs low exposure group comparison did. Of the 248 DMPs in the trend test, 80 (32%) had a *q*-value below 0.017, 217 (87.5%) had a *q*-value below 0.05, and 246 (99%) had a *q*-value below 0.1 in the high vs low exposure group comparison. The three top DMPs for the trend test were all among top-four in the high vs low exposure group comparison, situated in an intergenic region in chromosome 2 (cg03625947), protein-L-isoaspartate (D-aspartate) O-methyltransferase *(PCMT1)* and Rho GTPase activating protein 15 (*ARHGAP15*).

These observations indicated that the effect of PFAS exposure on DNA methylation might be gene- and dose-dependent.

3.2. DMRs in different PFAS exposure groups comparisons

We next investigated the associations between PFAS exposure and DMRs using the bumphunting method. We identified one DMR that was close to statistically significant, situated in the gene for S100 calcium binding protein A13 (*S100A13*), in the high vs. low exposure group comparison (FWER = 0.020). This DMR contained 15 CpGs and was negatively associated with PFAS exposure. This DMR was also among the top five DMRs in the high vs. medium exposure group comparison (FWER = 0.32) where it was negatively associated with PFAS exposure.

3.3. In silico functional analysis

We conducted *in silico* functional analyses to identify potential biological functions associated with the genes that harbored DMPs based on a *q-value* < 0.05 (N = 566 DMPs, of which 411 were annotated to known gene symbols, Supplemental Fig. S1). Top canonical pathways when considering all DMPs in each exposure group comparison together are shown in Fig. 2. Estrogen Receptor Signaling and cardiac hypertrophy signaling were the top significant canonical pathways (based on *p*-value from Fisher's exact test). Other top categories of interest for PFAS, based

Table 2

Differently methylated positions (ranked by *q*-value) determined in different exposure group comparisons and in the trend test.

CpG	Chr	Position[a]	Gene	Gene name	2^logFC (95% CI)[b]	*q*-value	Beta[c]	Trend test[d] β_1 (95% CI) and *q*-value
High vs. low exposure group[e]								
cg03625947	2	11,983,898	NA[f]		0.80 (0.75, 0.84)	<0.001	0.38	−0.17 (−0.21, −0.12), 0.00005
cg10469359	12	132,315,227	MMP17	Matrix metallopeptidase 17	0.81 (0.77, 0.86)	<0.001	0.04	−0.12 (−0.19, −0.05), 0.18
cg26779265	6	150,082,547	PCMT1	Protein-L-isoaspartate (D-aspartate) *O*-methyltransferase	0.82 (0.77, 0.86)	<0.001	0.25	−0.15 (−0.19, −0.10), 0.002
cg06008724	22	45,403,507	PHF21B	PHD finger protein 21B	0.49 (0.4, 0.61)	0.002	0.07	−0.50 (−0.69, −0.31), 0.024
cg19925435	2	144,440,441	ARHGAP15	Rho GTPase activating protein 15	0.84 (0.8, 0.88)	0.002	0.24	−0.13 (−0.16, −0.09), 0.002
cg23351738	6	31,589,926	SNORA38	Small nucleolar RNA, H/ACA box 38	1.38 (1.25, 1.52)	0.002	0.67	0.22 (0.13, 0.31), 0.053
cg20584474	6	1,515,696	NA		1.25 (1.17, 1.34)	0.002	0.88	0.16 (0.10, 0.22), 0.013
cg15998406	19	1,287,832	EFNA2	Ephrin A2	0.62 (0.53, 0.72)	0.002	0.25	−0.33 (−0.46, −0.21), 0.024
cg24655066	2	242,449,352	STK25	Serine/threonine kinase 25	0.79 (0.74, 0.85)	0.002	0.90	−0.17 (−0.22, −0.12), 0.003
cg01565037	10	74,715,059	PLA2G12B	Phospholipase A2 group XIIB	0.87 (0.84, 0.91)	0.002	0.81	−0.10 (−0.13, −0.06), 0.012
High vs. medium exposure group								
cg00613827	1	207,845,937	CR1L	Complement C3b/C4b receptor 1 like	1.85 (1.54, 2.23)	0.009	0.09	0.14 (0.004, 0.28), 0.52
cg27529004	2	237,490,808	ACKR3	Atypical chemokine receptor 3	0.87 (0.84, 0.91)	0.009	0.85	−0.07 (−0.11, −0.03), 0.17
cg01577980	7	116,412,971	MET	MET proto-oncogene, receptor tyrosine kinase	0.78 (0.72, 0.84)	0.012	0.88	−0.0003 (−0.09, 0.09), 1.00
cg02328102	2	187,988,552	NA		0.82 (0.77, 0.87)	0.012	0.77	−0.05 (−0.11, 0.01), 0.61
cg10155628	2	110,902,558	NPHP1	Nephrocystin 1	1.17 (1.11, 1.23)	0.012	0.76	0.10 (0.05, 0.15), 0.12
cg03686366	16	84,733,035	USP10	Ubiquitin-specific peptidase 10	0.84 (0.79, 0.89)	0.016	0.13	−0.06 (−0.12, −0.0003), 0.50
cg13236550	2	11,450,786	ROCK2	Rho-associated coiled-coil containing protein kinase 2	1.19 (1.12, 1.26)	0.016	0.87	0.07 (0.01, 0.12), 0.39
cg13425515	18	2,571,394	NDC80	NDC80, kinetochore complex component	1.19 (1.12, 1.26)	0.016	0.05	0.01 (−0.06, 0.08), 0.97
cg19805775	7	82,164,117	NA		0.81 (0.75, 0.87)	0.016	0.63	−0.01 (−0.09, 0.06), 0.95
cg09973148	2	37,899,355	CDC42EP3	CDC42 effector protein 3	1.27 (1.17, 1.37)	0.016	0.05	0.14 (0.04, 0.25), 0.34
cg16620537	5	140,306,054	PCDHA7	protocadherin alpha 7	0.86 (0.82, 0.91)	0.017	0.04	−0.05 (−0.11, −0.004), 0.49
Medium vs. low exposure group								
cg03314875	7	5,228,779	WIPI2	WD repeat domain, phosphoinositide interacting 2	1.19 (1.13, 1.26)	0.004	0.83	0.08 (0.02, 0.13), 0.33
cg08464140	7	5,197,343	NA		0.83 (0.79, 0.88)	0.004	0.70	−0.06 (−0.12, −0.01), 0.48
cg10469359	12	132,315,227	MMP17	Matrix metallopeptidase 17	0.83 (0.78, 0.88)	0.004	0.04	−0.12 (−0.19, −0.05), 0.18
cg13736369	3	46,775,569	NA		0.86 (0.83, 0.9)	0.004	0.90	−0.05 (−0.10, −0.0002), 0.54
cg24655422	14	95,429,934	NA		0.88 (0.85, 0.92)	0.011	0.62	−0.04 (−0.08, 0.01), 0.63
cg01577980	7	116,412,971	MET	MET proto-oncogene, receptor tyrosine kinase	1.27 (1.17, 1.37)	0.013	0.88	−0.0003 (−0.09, 0.09), 1.00
cg02631651	2	89,157,929	NA		0.80 (0.74, 0.86)	0.013	0.16	−0.11 (−0.18, −0.04), 0.27
cg03350491	20	44,987,255	SLC35C2	Solute carrier family 35 member C2	0.88 (0.85, 0.92)	0.013	0.21	−0.05 (−0.10, −0.01), 0.37
cg15575165	9	35,079,989	FANCG	Fanconi anemia complementation group G	0.68 (0.6, 0.78)	0.013	0.08	−0.07 (−0.19, 0.05), 0.77
cg25025310	1	37,091,601	NA		1.18 (1.12, 1.24)	0.013	0.84	0.04 (−0.01, 0.09), 0.61
cg20362335	1	205,028,130	CNTN2	contactin 2	1.14 (1.11, 1.19)	0.014	0.74	0.074 (0.028–0.12), 0.22
cg18495166	2	168,103,996	XIRP2	xin actin binding repeat containing 2	1.17 (1.11, 1.23)	0.017	0.69	0.11 (0.06, 0.15), 0.046
Trend test								

Table 2 (*continued*)

CpG	Chr	Position[a]	Gene	Gene name	2^logFC (95% CI)[b]	q-value	Beta[c]	Trend test[d] β_1 (95% CI) and q-value
cg03625947	2	11,983,898	NA					−0.17 (−0.21, −0.12), 0.00005
cg26779265	6	150,082,547	*PCMT1*	Protein-L-isoaspartate (D-aspartate) *O*-methyltransferase				−0.15 (−0.19, −0.10), 0.002
cg19925435	2	144,440,441	*ARHGAP15*	Rho GTPase activating protein 15				−0.13 (−0.16, −0.09), 0.002
cg24655066	2	242,449,352	*STK25*	Serine/threonine kinase 25				−0.17 (−0.22, −0.12), 0.003
cg02138218	1	175,035,502	*TNN*	tenascin N				(0.09 (0.06, 0.12), 0.003
cg18148659	15	65,953,468	*DENND4A*	DENN domain containing 4A				−0.11 (−0.14, −0.07), 0.003
cg26219179	2	182,011,089	*LOC101927156*	long intergenic non-protein coding RNA 1934				0.08 (0.06, 0.11), 0.003
cg16694239	1	160,179,710	*PEA15*	proliferation and apoptosis adaptor protein 15				0.09 (0.06, 0.12), 0.003
cg09157632	15	55,627,493	*PIGB*	phosphatidylinositol glycan anchor biosynthesis class B				−0.09 (−0.12, −0.06), 0.004
cg06978145	20	30,754,792	*TM9SF4*	transmembrane 9 superfamily member 4				−0.13 (−0.17, −0.09), 0.006

Abbreviations: Chr, chromosome; CI, confidence interval; q-value, False discovery rate (FDR)-adjusted *p*-value using the Benjamini-Hochberg method; FC, fold change.

[a] Position according to the Bioconductor package IlluminaHumanMethylationEPICanno.ilm10b4.hg19.

[b] 2^logFC, binary logarithmic fold change. LogFC denotes β_1 from the following robust regression model: M−value $= \beta_1 \times$ exposure group comparison $+ \beta_2 \times$ slide $+ \beta_3 \times$ estimated fraction CD4$^+$ T cells $+ \beta_4 \times$ estimated fraction CD8$^+$ T cells.

[c] Average methylation state, expressed as Beta-value, for all study participants, ranging from 0 to 1 (1 means fully methylated).

[d] Regression coefficients (β_1), 95% CI and q-values from trend test. β_1 from the following robust regression model: M−value $= \beta_1 \times$ exposure group (as a continuous variable) $+ \beta_2 \times$ slide $+ \beta_3 \times$ estimated fraction CD4 + T cells $+ \beta_4 \times$ estimated fraction CD8 + T cells.

[e] The exposure group denoted last is the reference group.

[f] NA, not annotated, i.e., the CpG is not present in any known gene.

on the literature, were Peroxisome proliferator-activated receptor alpha/Retinoid X receptor alpha (PPARα/RXRα) activation and telomerase signaling. Canonical pathway analyses for the three separate exposure group comparisons are shown in Supplemental Fig. S2. However, possibly due to the smaller number of DMPs included in the low vs. medium and high vs. medium exposure group comparisons, z-scores could not be calculated, meaning that no pattern of specific direction could be given for any pathway. In addition, there were few significant hits and the p-values were considerably weaker than in the analyses for the DMPs from the low vs. high exposure group comparison. For these two analyses, the HOTAIR regulatory pathway was the top hit. For the high vs. low exposure group comparison, z-scores could be calculated, and data were thus filtered for z-score, which was not possible to do for the other group comparisons. The top hits for the high vs. low exposure group comparison were similar to the top hits of the analysis for all DMPs.

Top diseases and biological functions when considering all DMPs in each exposure group comparison together are shown in Fig. 3. Cancer, organismal injury and abnormalities, gastrointestinal disease, endocrine system disorders, and reproductive system disease were among the top hits. Top diseases and biological functions for the three separate group comparisons are shown in Supplemental Fig. S3. Cancer, organismal injury and abnormalities, and gastrointestinal disease were among the top hits all three group comparisons.

We also performed a sensitivity analysis by including only DMPs based on $q < 0.017$ (data not shown), but then the z-scores for canonical pathway were not successfully calculated, neither for when considering exposure groups comparisons separately, nor for when considering all DMPs in each exposure group comparison together, meaning that no pattern of specific direction of could be given for any pathway. The reason for this may be a smaller number of genes included as well as a large shift in values of the most significant *p*-values in the canonical pathway analyses. For example, when including CpGs with *q*-values below 0.05 from all group comparisons, we observed the strongest significance of enriched canonical pathways in the range from –log(p-value) < 4.52 with identified z-scores, while when including CpGs with *q*-values below 0.017 from all group comparisons, we observed the

strongest association of an enriched canonical pathway in the range from –log(p-value) < 1.98 without any identified z-score (2.2-times stronger and reliable effects among the dataset with $q < 0.05$). Thus, we used $q < 0.05$ as cutoff in the *in silico* functional analysis.

3.4. PFAS exposure and epigenetic age acceleration

We investigated whether PFAS exposure is associated with epigenetic age acceleration. We noted a high correlation between the epigenetic age and chronological age in the study participants ($r_s = 0.94$, $p < 0.001$). However, we did not observe statistically significant differences in epigenetic age acceleration between the different exposure groups ($p = 0.43$, ANOVA; $p > 0.22$ for all post-hoc comparisons; Supplemental Table S2). Therefore, our results do not provide evidence supporting an association between PFAS exposure and epigenetic age acceleration.

4. Discussion

In this pilot study, we investigated the association between PFAS exposure and DNA methylation in women with a PFAS exposure profile dominated by PFOS and PFHxS from drinking water. We found that PFAS exposure was associated with methylation of specific sites and regions. We noted that hypomethylation was more common than hypermethylation in the high vs. low exposure group comparison. *In silico* functional analyses suggested that genes with altered DNA methylation were related to pathways such as estrogen receptor signaling, cardiac hypertrophy signaling, telomerase signaling and PPARα/RXRα activation as well as diseases and biological functions such as cancer, endocrine system disorders and reproductive system disease. Contrary to our hypothesis, we did not note any association between PFAS exposure and epigenetic age acceleration. These observations suggest that DNA methylation may be a mechanism of PFAS toxicity, although future studies are needed to determine if PFAS-induced changes in DNA methylation mediate the association between PFAS exposure and adverse health outcomes.

We detected statistically significant DMPs (among these, *MMP17, XIRP2* and *PHF21B* were top hits in more than one exposure group
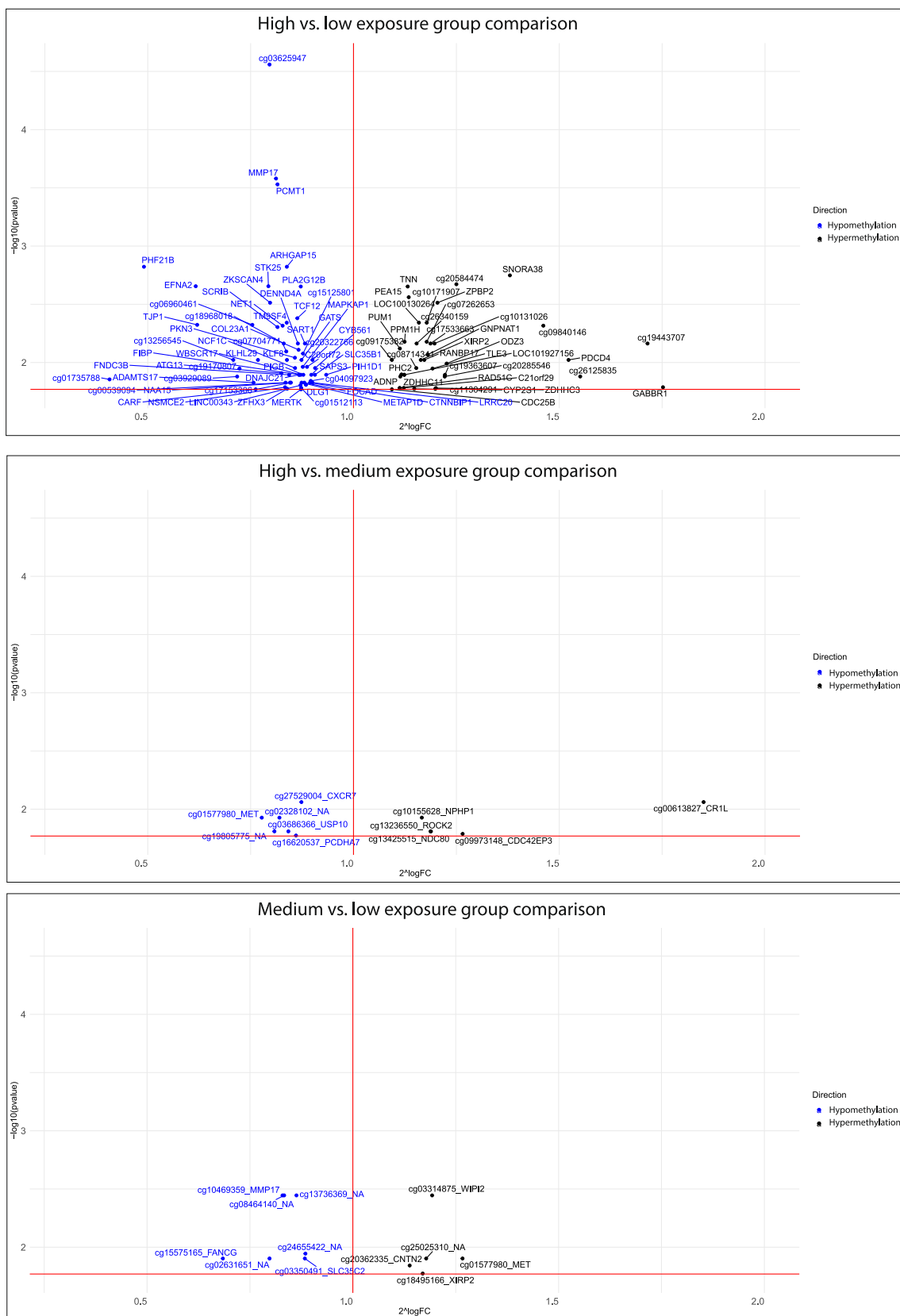
Fig. 1. Volcano plots showing the *q*-value (for DMPs showing statistical significance, $q < 0.017$) versus magnitude of change (2ˆlogFC) for the different exposure group comparisons. (A) High vs. low exposure group comparison; (B) high vs. medium exposure group comparison; and (C) medium vs. low exposure group comparison. The red line at the x-axis denotes the statistical significance (-log10(0.017)) and the red line at the y-axis denotes a 2ˆlogFC of 1 (no change at either direction). For B) and C) each dot is labelled with corresponding CpG ID and gene name (the gene name is replaced with NA, when the CpG is not annotated to a gene). For A) each dot is labelled with corresponding gene name only, but when the CpG is not annotated to a gene, CpG ID is added instead. (For interpretation of the references to colour in this figure legend, the reader is referred to the web version of this article.)
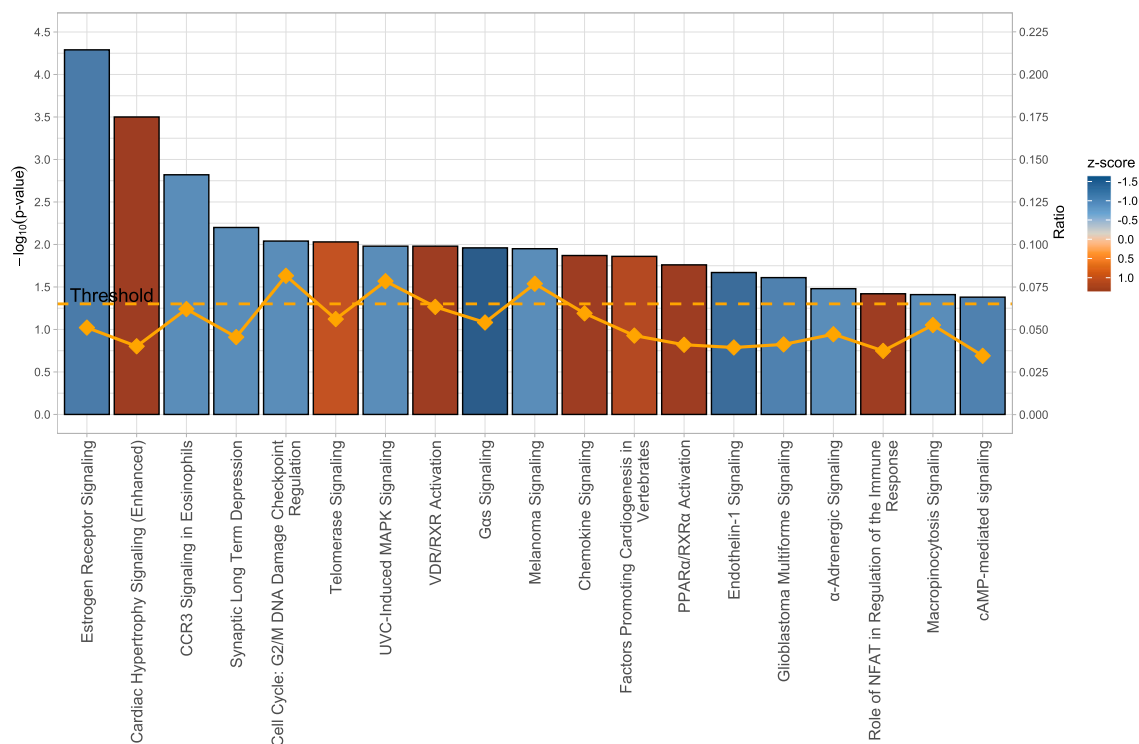
Fig. 2. Top canonical pathways determined by the Ingenuity Pathway Analysis (IPA) of genes with differently methylated positions (based on *q* < 0.050) in all group comparisons. X-axis, canonical pathways; primary y-axis (left, bar chart), the logarithm of *p*-value from the right-tailed Fisher's exact test; secondary y-axis (right, line chart), ratio. The red and blue bars indicate predicted pathway activation or inhibition, respectively, calculated based on the z-score. The dashed line denoted "Threshold" indicates the –log10 for the significance *p*-value of 0.05. The ratio describes the number of genes from the list generated in the course of DMP analysis that map to the pathway to the total number of genes that map to the pathway (from the IPA library of canonical pathways). (For interpretation of the references to colour in this figure legend, the reader is referred to the web version of this article.)
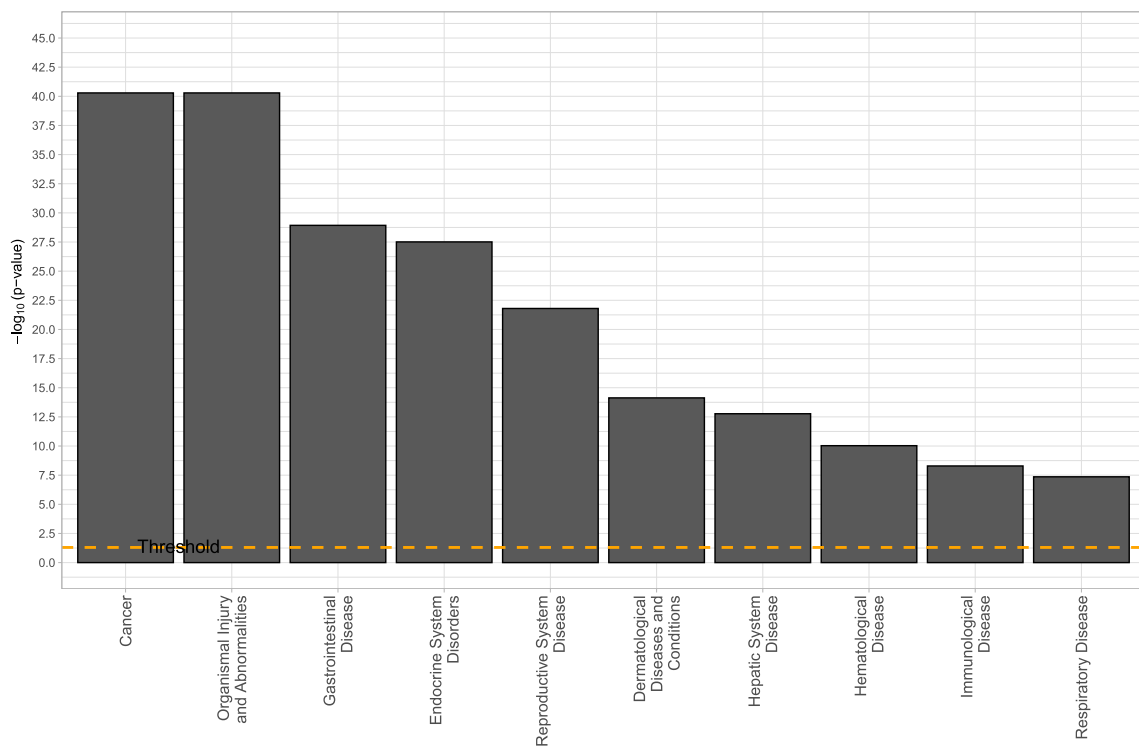
Fig. 3. Top diseases and biological functions revealed by the Ingenuity Pathway Analysis of genes with differently methylated positions (based on *q* < 0.050) in all group comparisons. X-axis, statistically significant diseases and biological functions based on the *p*-value of right-tailed Fisher's exact test, reflecting the likelihood that the association between a set of genes in the dataset and a related biological function is significant. Y-axis, logarithm of Fisher's exact test *p*-value. The dashed line denoted "Threshold" indicates the –log10 for the significance p-value of 0.05.

comparison and with the same directions in both group comparisons) and one near-statistically significant DMR (*S100A13*) in exposure group comparisons. *MMP17* was associated with PFAS exposure in more than one exposure group comparison and was hypomethylated with increasing PFAS exposure. *MMP17* is involved in the breakdown of extracellular matrix during normal physiological processes, such as embryonic development, reproduction, and tissue remodeling, as well as in disease processes, such as arthritis and metastasis (NCBI gene [accessed 3 June 2020], https://www.ncbi.nlm.nih.gov/gene/). *XIRP2* was hypermethylated with increasing PFAS exposure. It is strongly expressed in heart and has been associated with e.g. cardiac morphology, function, and disease (NCBI gene [accessed 3 June 2020]) (Wang et al. 2014). *PHF21B*, which appeared among top DMPs in two exposure group comparisons, is strongly expressed in the brain, and has been associated with major depressive disorder, modulation of stress response, and cancer (NCBI gene [accessed 3 June 2020]).

The strongest associations between DNA methylation and PFAS exposure, according to *q*-value, were seen in the high vs. low exposure group comparison. The top DMPs in the high vs. low exposure group comparison were similar as the top DMPs in the trend test. Two top DMPs that were annotated to genes in both these analyses were *PCMT1* and *ARHGAP15*. *PCMT1* catalyzes the methyl esterification of L-iso-aspartyl and D-aspartyl residues in peptides and proteins that result from spontaneous decomposition of normal L-aspartyl and L-asparaginyl residues. It plays a role in the repair and/or degradation of damaged proteins (NCBI gene [accessed 21 August 2020]). *ARHGAP15* is a RHO GTPase-activating protein (Seoh et al., 2003), which has been associated with different types of cancers, such as breast cancer and colorectal cancer (Pan et al. 2018, Takagi et al. 2018).

The DMR analysis revealed that *S100A13* was near-statistically significantly negatively associated with PFAS in the high vs. low exposure group comparison. S100 proteins are localized in the cytoplasm and nucleus in many cells and are involved in the regulation of several cellular processes, such as cell cycle progression and differentiation (Cao et al. 2010). The *S100A13* gene is widely expressed in various tissue types, and highly expressed in the thyroid gland (Ridinger et al. 2000). *S100A13* has been suggested to influence the development and metastasis of cancer, and previous studies have shown that *S100A13* influences the prognosis of several different types of cancers, such as ovarian cancer (Tian et al. 2017), breast cancer (Chen et al. 2017) and thyroid cancer (Zhong et al. 2016). In the current study, DMPs were mainly identified while comparing the high exposure group with the low exposure group. This indicates that the threshold exposure for attaining an epigenetic effect may be fairly high. We saw a similar pattern in a previous study on the effect of PFAS and microRNA expression, including women from the same study population, in which alterations in serum microRNA levels were mainly seen when comparing the low and high exposure group samples (Xu et al. 2020). However, in the current study, samples of relatively few participants from each exposure group were analyzed, and the study may be underpowered.

None of the identified top DMPs or DMRs were located in genes that have previously been associated with DNA methylation upon PFAS exposure among newborns or men (Kingsley et al. 2017; Leung et al. 2018; Miura et al. 2018; van den Dungen et al. 2017). This may partly be explained by sex differences (El-Maarri et al. 2007; Liu et al. 2010) or that DNA methylation differ between newborns and adults (Day et al. 2013, Sikdar et al. 2019). Additionally, the serum PFAS levels in the present study, especially PFOS and PFHxS, were much higher than in the other studies (e.g. the median PFOS in the high exposure group was 230 ng/mL in the present study, compared to less than 10 ng/mL in the above studies). Possibly, the inconsistencies between studies may indicate a dose-dependent pattern of differential methylation.

In silico functional analysis suggested that the top canonical pathways for all DMPs (based on a cut-off of $q < 0.05$) were estrogen receptor signaling and cardiac hypertrophy signaling. Estrogen receptor signaling was also a top canonical pathway when comparing DMPs in

the low vs. high exposure group comparison. Given that PFAS are known endocrine disrupting chemicals, the interaction of PFAS with the estrogen and/or androgen receptor could also be the underlying mechanism of toxicity (Kjeldsen and Bonefeld-Jorgensen, 2013; Bonefeld-Jørgensen et al., 2014). Rosen et al. (2017) have suggested that some genes in PFAS-treated animals were probably up- or down-regulated due to suppression of transactivation of the constitutive activated receptor, estrogen receptor alpha, and/or *PPARγ*. Associations between PFOS or PFOA exposure and cardiovascular diseases have been noted in some studies (Donat-Vargas et al. 2019; Huang et al. 2018; Shankar et al. 2012), but the epidemiological evidence is hitherto considered weak (EFSA 2018, EFSA 2020).

The canonical pathway analysis also suggested PPARα/RXRα activation as an enriched pathway. Peroxisome proliferator-activated receptor alpha (PPARα) forms heterodimers with Retinoid X receptor alpha (RXRα) and modulates the function of many target genes (Qi et al. 2000). PPARα is activated by endogenous ligands and evidence from *in vivo* and *in vitro* studies show that many PFAS act as ligands of PPARα in rodents and in human cells (Rosen et al. 2008; Vanden Heuvel et al. 2006). In our previous study, involving the same cohort as that analyzed in the current study, we identified *PPARα* as a possible target gene of microRNAs downregulated in serum with increasing PFAS exposure (Xu et al. 2020). PPARα is highly expressed in the liver and plays a prominent role in lipid regulation (Reddy & Hashimoto. 2001; Kersten and Stienstra. 2017). Given the fact that serum PFOS and PFOA have been associated with lipid metabolism (Sakr et al. 2007; Steenland et al. 2009), the capacity of PFAS to transactivate PPARα may be an important intermediate step through regulating lipid metabolism in humans.

Another of the top canonical pathways detected by the *in silico* analysis was telomerase signaling. Telomerase is the enzyme responsible for maintenance of telomere length. Telomere length is a marker of cellular aging, since telomeres are shortened with every cell division, eventually reaching a length that triggers cell senescence. Studies regarding PFAS exposure and leukocyte telomere length have given varied results; PFOS exposure was positively associated with telomere length in leukocytes among adults (Huang et al. 2019), negatively associated with telomere length in leukocytes among female newborns (no association in male newborns) (Liu et al., 2018a, 2018b), and no association was observed in leukocytes in a longitudinal study of childbearing women (Zota et al. 2018).

In silico analysis also suggested enrichment of genes associated with health outcomes, such as cancer, gastrointestinal disease, endocrine system disorders, and reproductive system disease. PFAS are endocrine disruptors, and epidemiological studies have reported associations between PFAS exposure and cancer incidence (Barry et al. 2013; Mancini et al. 2020), and changes in thyroid function in pregnant women (Ballesteros et al. 2017; Berg et al. 2015). However, the existing evidence from epidemiological studies is insufficient for making conclusions about PFAS carcinogenicity or toxicity in the endocrine system or reproductive system (EFSA 2018, EFSA 2020).

We did not find any association between PFAS exposure and epigenetic age acceleration in the current study. It could be due to the fact that epigenetic age was strongly correlated with chronological age, and thus, provided no additional information beyond the latter. Additionally, menopausal status has been suggested to be associated with both PFAS serum levels (because of reduced PFAS loss via menses) (Dhingra et al. 2017; Ding et al. 2020; Ruark et al. 2017) and biological aging (because of estrogen deficiency) (Wilkinson and Hardman 2017). However, most likely, the menopausal status is not a confounder in the current study since the mean age for menopause in Sweden is approximately 50 years (Rödström et al. 2005) and the current study involved women representing a narrow age span of 20–47 years. Interestingly, one of the top canonical pathways detected by the *in silico* analysis, telomerase signaling (as mentioned above), is tightly connected to telomere length, another indicator of biological aging. It may therefore be plausible that PFAS exposure influence aging by affecting telomere length. However,

as discussed above, previous studies regarding PFAS exposure and leukocyte telomere length have given varied results and further studies are needed to evaluate how PFAS exposure is related to telomere length.

This is a pilot study and thus limited by the small study size. However, its strength is a wide PFAS exposure range of the analyzed groups, ranging from the general population background levels to very high levels, especially for PFOS and PFHxS. For instance, the median levels of PFOS in the medium and high exposure group were more than ten-fold or even higher than that reported in other populations who also exposed through drinking water, mainly originated from industrial emissions (Frisbee et al. 2009; Hölzer et al. 2008; Ingelido et al. 2018). Considering the relatively small sample size in this with healthy general population, we did not aim to evaluate the possible associations between PFAS exposure, DNA methylation, and further phenotypic outcomes *in vivo*. Another limitation of the current study is the assessment of DNA methylation in the blood instead of specific tissues targeted by PFAS (such as the liver). Future studies with larger sample sizes are needed to validate the findings and to further investigate whether PFAS-associated changes in DNA methylation underlie potential phenotypic changes and/or adverse health effects of PFAS.

Collectively, our pilot study in a female cohort indicates that PFAS exposure is associated with DNA methylation changes at specific sites, and modulation of DNA methylation may thus be a suggestive mechanism of PFAS toxicity. Further studies coupling the PFAS-associated changes in DNA methylation to phenotypical effects of PFAS are needed to evaluate if DNA methylation as a mechanism of toxicity or if it is merely an effect of exposure. This study has also highlighted potential associations between PFAS exposure and methylation changes of genes associated with pathways such as estrogen receptor signaling, cardiac hypertrophy signaling, telomerase signaling and PPARα/RXRα activation pathways.

CRediT authorship contribution statement

Yiyi Xu: Methodology, Formal analysis, Writing - original draft, Writing - review & editing. **Simona Jurkovic-Mlakar:** Visualization, Formal analysis, Writing - review & editing. **Christian H. Lindh:** Resources, Writing - review & editing. **Kristin Scott:** Resources, Investigation, Writing - review & editing. **Tony Fletcher:** Resources, Writing - review & editing. **Kristina Jakobsson:** Conceptualization, Funding acquisition, Writing - review & editing. **Karin Engström:** Conceptualization, Methodology, Formal analysis, Writing - original draft, Project administration, Supervision, Funding acquisition, Writing - review & editing.

Declaration of Competing Interest

The authors declare that they have no known competing financial interests or personal relationships that could have appeared to influence the work reported in this paper.

Appendix A. Supplementary data

Supplementary data to this article can be found online at https://doi.org/10.1016/j.envint.2020.106148.

References

Baccarelli, A., Bollati, V., 2009. Epigenetics and environmental chemicals. Curr. Opin. Pediatr. 21 (2), 243–251. https://doi.org/10.1097/mop.0b013e32832925cc.

Ballesteros, V., Costa, O., Iniguez, C., Fletcher, T., Ballester, F., Lopez-Espinosa, M.J., 2017. Exposure to perfluoroalkyl substances and thyroid function in pregnant women and children: A systematic review of epidemiologic studies. Environ. Int. 99, 15–28. https://doi.org/10.1016/j.envint.2016.10.015.

Banzhaf, S., Filipovic, M., Lewis, J., Sparrenbom, C.J., Barthel, R.J., 2017. A review of contamination of surface-, ground-, and drinking water in sweden by perfluoroalkyl and polyfluoroalkyl substances (PFASs). Ambio. 46 (3), 335–346. https://doi.org/10.1007/s13280-016-0848-8.

Barry, V., Winquist, A., Steenland, K., 2013. Perfluorooctanoic acid (PFOA) exposures and incident cancers among adults living near a chemical plant. Environ. Health Perspect. 121 (11–12), 1313–1318. https://doi.org/10.1289/ehp.1306615.

Berg, V., Nøst, T.H., Hansen, S., et al., 2015. Assessing the relationship between perfluoroalkyl substances, thyroid hormones and binding proteins in pregnant women; a longitudinal mixed effects approach. Environ. Int. 77, 63–69. https://doi.org/10.1016/j.envint.2015.01.007.

Blake, B.E., Pinney, S.M., Hines, E.P., Fenton, S.E., Ferguson, K.K., 2018. Associations between longitudinal serum perfluoroalkyl substance (PFAS) levels and measures of thyroid hormone, kidney function, and body mass index in the Fernald Community Cohort. Environ. Pollut. 242 (Pt A), 894–904. https://doi.org/10.1016/j.envpol.2018.07.042.

Bonefeld-Jørgensen, E.C., Ghisari, M., Wielsøe, M., Bjerregaard-Olesen, C., Kjeldsen, L.S., Long, M., 2014. Biomonitoring and hormone-disrupting effect biomarkers of persistent organic pollutants in vitro and ex vivo. Basic Clin. Pharmacol. Toxicol. 115 (1), 118–128. https://doi.org/10.1111/bcpt.12263.

Cao, R., Yan, B., Yang, H., Zu, X., Wen, G., Zhong, J., 2010. Effect of human S100A13 gene silencing on FGF-1 transportation in human endothelial cells. J. Formos. Med. Assoc. 109 (9), 632–640. https://doi.org/10.1016/S0929-6646(10)60103-9.

Chen, A., Wang, L., Li, B.Y., et al., 2017. Reduction in Migratory Phenotype in a Metastasized Breast Cancer Cell Line via Downregulation of S100A4 and GRM3. Sci. Rep. 7, 1, 3459. Published 2017 Jun 14. http://doi.org/10.1038/s41598-017-03811-9.

Curtis, S.W., Cobb, D.O., Kilaru, V., Terrell, M.L., Marder, M.E., Barr, D.B., et al., 2019. Environmental exposure to polybrominated biphenyl (PBB) associates with an increased rate of biological aging. Aging (Albany NY). 11 (15), 5498–5517. https://doi.org/10.18632/aging.102134.

Day, K., Waite, L.L., Thalacker-Mercer, A., et al., 2013. Differential DNA methylation with age displays both common and dynamic features across human tissues that are influenced by CpG landscape. Genome Biol. 14 (9), R102. https://doi.org/10.1186/gb-2013-14-9-r102.

Dhingra, R., Winquist, A., Darrow, L.A., Klein, M., Steenland, K., 2017. A study of reverse causation: Examining the associations of perfluorooctanoic acid serum levels with two outcomes. Environ. Health Perspect. 125 (3), 416–421. https://doi.org/10.1289/EHP273.

Ding, N., Harlow, S.D., Batterman, S., Mukherjee, B., Park, S.K., 2020. Longitudinal trends in perfluoroalkyl and polyfluoroalkyl substances among multiethnic midlife women from 1999 to 2011: The study of women' s health across the Nation. Environ. Int. 135, 105381 https://doi.org/10.1016/j.envint.2019.105381.

Donat-Vargas, C., Bergdahl, I.A., Tornevi, A., Wennberg, M., Sommar, J., Koponen, J., et al., 2019. Associations between repeated measure of plasma perfluoroalkyl substances and cardiometabolic risk factors. Environ. Int. 124, 58–65. https://doi.org/10.1016/j.envint.2019.01.007.

Drinking water inspectorate. Guidance on the water supply (water quality) regulations 2000 specific to PFOS (perfluorooctane sulphonate) and PFOA (perfluorooctanoic acid) concentarations in drinking water. October 2009. Available: http://www.dwi.gov.uk/stakeholders/information-letters/2009/10_2009annex.pdf. Accessed on 2020-06-01.

EFSA. 2018. Risk to human health related to the presence of perfluorooctane sulfonic acid and perfluorooctanoic acid in food. EFSA Journal 16:e05194. Available: https://efsa.onlinelibrary.wiley.com/doi/epdf/10.2903/j.efsa.2018.5194. Accessed on 2020-06-25.

EFSA. 2020. Public consultation on the draft scientific opinion on the risks to human health related to the presence of perfluoroalkyl substances in food. Available from https://www.efsa.europa.eu/sites/default/files/consultation/consultation/PFAS_Draft_Opinion_for_public_consultation_Part I.pdf. Accessed on 2020-06-01. (Recently this is the draft).

El-Maarri, O., Becker, T., Junen, J., et al., 2007. Gender specific differences in levels of DNA methylation at selected loci from human total blood: a tendency toward higher

methylation levels in males. Hum. Genet. 122 (5), 505–514. https://doi.org/10.1007/s00439-007-0430-3.

Florath, I., Butterbach, K., Müller, H., Bewerunge-Hudler, M., Brenner, H., 2014. Cross-sectional and longitudinal changes in DNA methylation with age: an epigenome-wide analysis revealing over 60 novel age-associated CpG sites. Hum. Mol. Genet. 23, 1186–1201. https://doi.org/10.1093/hmg/ddt531.

Fortin, J.-P., Triche Jr, T.J., Hansen, K.D., 2017. Preprocessing, normalization and integration of the illumina humanmethylationepic array with minfi. Bioinformatics. 33 (4), 558–560. https://doi.org/10.1093/bioinformatics/btw691.

Frisbee, S.J., Brooks Jr, A.P., Maher, A., Flensborg, P., Arnold, S., Fletcher, T., et al., 2009. The C8 health project: Design, methods, and participants. Environ. Health Perspect. 117, 1873–1882. https://doi.org/10.1289/ehp.0800379.

Guelfo, J.L., Adamson, D.T., 2018. Evaluation of a national data set for insights into sources, composition, and concentrations of per-and polyfluoroalkyl substances (PFASs) in US drinking water. Environ. Pollut. 236, 505–513. https://doi.org/10.1016/j.envpol.2018.01.066.

Guerrero-Preston, R., Goldman, L.R., Brebi-Mieville, P., et al., 2010. Global DNA hypomethylation is associated with in utero exposure to cotinine and perfluorinated alkyl compounds. Epigenetics. 5 (6), 539–546. https://doi.org/10.4161/epi.5.6.12378.

Horvath, S., 2013. DNA methylation age of human tissues and cell types [published correction appears in Genome Biol. 2015;16:96]. Genome Biol. 14, 10, R115. http://doi.org/10.1186/gb-2013-14-10-r115.

Horvath, S., Oshima, J., Martin, G.M., Lu, A.T., Quach, A., Cohen, H., et al., 2018. Epigenetic clock for skin and blood cells applied to hutchinson gilford progeria syndrome and *ex vivo* studies. Aging (Albany NY). 10 (7), 1758–1775. https://doi.org/10.18632/aging.101508.

Houseman, E.A., Accomando, W.P., Koestler, D.C., Christensen, B.C., Marsit, C.J., Nelson, H.H., et al., 2012. DNA methylation arrays as surrogate measures of cell mixture distribution. BMC Bioinformatics. 13, 86. https://doi.org/10.1186/1471-2105-13-86.

Huang, H., Wang, Q., He, X., Wu, Y., Xu, C., 2019. Association between polyfluoroalkyl chemical concentrations and leucocyte telomere length in US adults. Sci. Total Environ. 653, 547–553. https://doi.org/10.1016/j.scitotenv.2018.10.400.

Huang, M., Jiao, J., Zhuang, P., Chen, X., Wang, J., Zhang, Y., 2018. Serum polyfluoroalkyl chemicals are associated with risk of cardiovascular diseases in national US population. Environ. Int. 119, 37–46. https://doi.org/10.1016/j.envint.2018.05.051.

Hölzer, J., Midasch, O., Rauchfuss, K., Kraft, M., Reupert, R., Angerer, J., et al., 2008. Biomonitoring of perfluorinated compounds in children and adults exposed to perfluorooctanoate-contaminated drinking water. Environ. Health Perspect. 116, 651–657. https://doi.org/10.1289/ehp.11064.

Ingelido, A.M., Abballe, A., Gemma, S., Dellatte, E., Iacovella, N., De Angelis, G., et al., 2018. Biomonitoring of perfluorinated compounds in adults exposed to contaminated drinking water in the Veneto region Italy. Environ. Int. 110, 149–159. https://doi.org/10.1016/j.envint.2017.10.026.

Johansson, A., Enroth, S., Gyllensten, U., 2013. Continuous Aging of the Human DNA Methylome Throughout the Human Lifespan. PLoS One. 27;86, e67378. https://doi.org/10.1371/journal.pone.0067378.

Kersten, S., Stienstra, R., 2017. The role and regulation of the peroxisome proliferator activated receptor alpha in human liver. Biochimie. 136, 75–84. https://doi.org/10.1016/j.biochi.2016.12.019.

Kingsley, S.L., Kelsey, K.T., Butler, R., Chen, A., Eliot, M.N., Romano, M.E., et al., 2017. Maternal serum PFOA concentration and DNA methylation in cord blood: A pilot study. Environ. Res. 158, 174–178. https://doi.org/10.1016/j.envres.2017.06.013.

Kjeldsen, L.S., Bonefeld-Jorgensen, E.C., 2013. Perfluorinated compounds affect the function of sex hormone receptors. Environ. Sci. Pollut. Res. Int. 20, 8031–8044.

Knox, S.S., Jackson, T., Javins, B., Frisbee, S.J., Shankar, A., Ducatman, A.M., 2011. Implications of early menopause in women exposed to perfluorocarbons. J. Clin. Endocrinol. Metab. 96 (6), 1747–1753. https://doi.org/10.1210/jc.2010-2401.

Lauss, M., Visne, I., Kriegner, A., Ringnér, M., Jönsson, G., Höglund, M., 2013. Monitoring of technical variation in quantitative high-throughput datasets. Cancer Inform. 12, 193–201. Published 2013 Sep 23. http://doi.org/10.4137/CIN.S12862.

Leung, Y.K., Ouyang, B., Niu, L., Xie, C., Ying, J., Medvedovic, M., et al., 2018. Identification of sex-specific DNA methylation changes driven by specific chemicals in cord blood in a faroese birth cohort. Epigenetics. 13 (3), 290–300. https://doi.org/10.1080/15592294.2018.1445901.

Li, Y., Fletcher, T., Mucs, D., Scott, K., Lindh, C.H., Tallving, P., et al., 2018. Half-lives of pfos, pfhxs and pfoa after end of exposure to contaminated drinking water. Occup. Environ. Med. 75 (1), 46–51. https://doi.org/10.1136/oemed-2017-104651.

Lind, P.M., Salihovic, S., Lind, L., 2018. High plasma organochlorine pesticide levels are related to increased biological age as calculated by DNA methylation analysis. Environ. Int. 113, 109–113. https://doi.org/10.1016/j.envint.2018.01.019.

Liu, C.Y., Chen, P.C., Lien, P.C., Liao, Y.P., 2018a. Prenatal perfluorooctyl sulfonate exposure and alu DNA hypomethylation in cord blood. Int. J. Environ. Res. Public Health. 15 (6), pii: E1066. https://doi.org/10.3390/ijerph15061066.

Liu, H., Chen, Q., Lei, L., et al., 2018b. Prenatal exposure to perfluoroalkyl and polyfluoroalkyl substances affects leukocyte telomere length in female newborns. Environ. Pollut. 235, 446–452. https://doi.org/10.1016/j.envpol.2017.12.095.

Liu, J., Morgan, M., Hutchison, K., Calhoun, V.D., 2010. A study of the influence of sex on genome wide methylation. PLoS One. 5 (4), e10028 https://doi.org/10.1371/journal.pone.0010028.

Livsmedelsverket. Riskhanteringsrapport (2016-02-09). Risker vid förorening av dricksvatten med PFAS. Available: https://www.livsmedelsverket.se/globalassets/produktion-handel-kontroll/dricksvatten/riskhanteringsrapport-pfas-160229.pdf. Accessed on 2020-06-01. (In Swedish).

Mancini, F.R., Cano-Sancho, G., Gambaretti, J., Marchand, P., Boutron-Ruault, M.C., Severi, G., Arveux, P., Antignac, J.P., Kvaskoff, M., 2020. Perfluorinated alkylated substances serum concentration and breast cancer risk: Evidence from a nested case-control study in the French E3N cohort. Int. J. Cancer. 146 (4), 917–928. https://doi.org/10.1002/ijc.32357.

Marioni, R.E., Shah, S., McRae, A.F., Chen, B.H., Colicino, E., Harris, S.E., et al., 2015a. DNA methylation age of blood predicts all-cause mortality in later life. Genome Biol. 16, 25. https://doi.org/10.1186/s13059-015-0584-6.

Marioni, R.E., Shah, S., McRae, A.F., Ritchie, S.J., Muniz-Terrera, G., Harris, S.E., et al., 2015b. The epigenetic clock is correlated with physical and cognitive fitness in the Lothian Birth Cohort 1936. Int. J. Epidemiol. 44 (4), 1388–1396. https://doi.org/10.1093/ije/dyu277.

Maunakea, A.K., Chepelev, I., Zhao, K., 2010. Epigenome mapping in normal and disease States. Circ. Res. 107 (3), 327–339. https://doi.org/10.1161/CIRCRESAHA.110.222463.

McCarthy, N.S., Melton, P.E., Cadby, G., et al., 2014. Meta-analysis of human methylation data for evidence of sex-specific autosomal patterns. BMC Genomics. 15 (1), 981. https://doi.org/10.1186/1471-2164-15-981.

Miura, R., Araki, A., Miyashita, C., Kobayashi, S., Kobayashi, S., Wang, S.L., et al., 2018. An epigenome-wide study of cord blood DNA methylations in relation to prenatal perfluoroalkyl substance exposure: The Hokkaido Study. Environ. Int. 115, 21–28. https://doi.org/10.1016/j.envint.2018.03.004.

NCBI Gene [Internet]. Bethesda (MD): National Library of Medicine (US), National Center for Biotechnology Information; 2004 – [cited 20200603]. Available from: https://www.ncbi.nlm.nih.gov/gene/.

Pan, S., Deng, Y., Fu, J., et al., 2018. Decreased expression of ARHGAP15 promotes the development of colorectal cancer through PTEN/AKT/FOXO1 axis. Cell Death Dis. 9, 6, 673. Published 2018 Jun 4. http://doi.org/10.1038/s41419-018-0707-6.

Qi, C., Zhu, Y., Reddy, J.K., 2000. Peroxisome proliferator-activated receptors, coactivators, and downstream targets. Cell Biochem. Biophys. 32, Spring, 187–204. http://doi.org/10.1385/cbb:32:1-3:187.

Reddy, J.K., Hashimoto, T., 2001. Peroxisomal beta-oxidation and peroxisome proliferator-activated receptor alpha: an adaptive metabolic system. Annu. Rev. Nutr. 21, 193–230. https://doi.org/10.1146/annurev.nutr.21.1.193.

Ridinger, K., Schäfer, B.W., Durussel, I., Cox, J.A., Heizmann, C.W., 2000. S100A13. Biochemical characterization and subcellular localization in different cell lines. J. Biol. Chem. 275 (12), 8686–8694. https://doi.org/10.1074/jbc.275.12.8686.

Rosen, M.B., Das, K.P., Rooney, J., Abbott, B., Lau, C., Corton, J.C., 2017. PPARα-independent transcriptional targets of perfluoroalkyl acids revealed by transcript profiling. Toxicology. 387, 95–107. https://doi.org/10.1016/j.tox.2017.05.013.

Rosen, M.B., Lee, J.S., Ren, H., Vallanat, B., Liu, J., Waalkes, M.P., et al., 2008. Toxicogenomic dissection of the perfluorooctanoic acid transcript profile in mouse liver: Evidence for the involvement of nuclear receptors PPARα and CAR. Toxicol. Sci. 103 (1), 46–56. https://doi.org/10.1093/toxsci/kfn025.

Ruark, C.D., Song, G., Yoon, M., Verner, M.A., Andersen, M.E., et al., 2017. Quantitative bias analysis for epidemiological associations of perfluoroalkyl substance serum concentrations and early onset of menopause. Environ. Int. 99, 245–254. https://doi.org/10.1016/j.envint.2016.11.030.

Rödström, K., Bengtsson, C., Lissner, L., Björkelund, C., 2005. Reproducibility of self-reported menopause age at the 24-year follow-up of a population study of women in Göteborg Sweden. Menopause. 12 (3), 275–280. https://doi.org/10.1097/01.gme.0000135247.11972.b3.

Sakr, C.J., Kreckmann, K.H., Green, J.W., Gillies, P.J., Reynolds, J.L., Leonard, R.C., 2007. Cross-sectional study of lipids and liver enzymes related to a serum biomarker of exposure (ammonium perfluorooctanoate or APFO) as part of a general health survey in a cohort of occupationally exposed workers. J. Occup. Environ. Med. 49 (10), 1086–1096. https://doi.org/10.1097/JOM.0b013e318156eca3.

Seoh, M.L., Ng, C.H., Yong, J., Lim, L., Leung, T., 2003. ArhGAP15, a novel human RacGAP protein with GTPase binding property. FEBS Lett. 539 (1–3), 131–137. https://doi.org/10.1016/s0014-5793(03)00213-8.

Shankar, A., Xiao, J., Ducatman, A., 2012. Perfluorooctanoic acid and cardiovascular disease in US adults. Arch. Intern. Med. 172 (18), 1397–1403. https://doi.org/10.1001/archinternmed.2012.3393.

Sikdar, S., Joehanes, R., Joubert, B.R., et al., 2019. Comparison of smoking-related DNA methylation between newborns from prenatal exposure and adults from personal smoking. Epigenomics. 11 (13), 1487–1500. https://doi.org/10.2217/epi-2019-0066.

Steenland, K., Tinker, S., Frisbee, S., Ducatman, A., Vaccarino, V., 2009. Association of perfluorooctanoic acid and perfluorooctane sulfonate with serum lipids among adults living near a chemical plant. Am. J. Epidemiol. 170 (10), 1268–1278. https://doi.org/10.1093/aje/kwp279.

Takagi, K., Miki, Y., Onodera, Y., et al., 2018. ARHGAP15 in Human Breast Carcinoma: A Potent Tumor Suppressor Regulated by Androgens. Int. J. Mol. Sci. 2018;19(3):804. Published 2018 Mar 10. http://doi.org/10.3390/ijms19030804.

Thomas, S., Bonchev, D., 2010. A survey of current software for network analysis in molecular biology. Hum. Genomics. 4 (5), 353–360. https://doi.org/10.1186/1479-7364-4-5-353.

Tian, T., Li, X., Hua, Z., et al., 2017. S100A1 promotes cell proliferation and migration and is associated with lymph node metastasis in ovarian cancer. Discov. Med. 23 (127), 235–245.

van den Dungen, M.W., Murk, A.J., Kampman, E., Steegenga, W.T., Kok, D.E., 2017a. Association between DNA methylation profiles in leukocytes and serum levels of persistent organic pollutants in Dutch men. Environ. Epigenet. 3,1, dvx001. http://doi.org/10.1093/eep/dvx001.

Vanden Heuvel, J.P., Thompson, J.T., Frame, S.R., Gillies, P.J., 2006. Differential activation of nuclear receptors by perfluorinated fatty acid analogs and natural fatty

acids: A comparison of human, mouse, and rat peroxisome proliferator-activated receptor-alpha,-beta, and-gamma, liver X receptor-beta, and retinoid X receptor-alpha. Toxicol. Sci. 92 (2), 476–489. https://doi.org/10.1093/toxsci/kfl014.

Wang, Q., Lin, J.L., Erives, A.J., Lin, C.I., Lin, J.J., 2014. New insights into the roles of Xin repeat-containing proteins in cardiac development, function, and disease. Int. Rev. Cell Mol. Biol. 310, 89–128. https://doi.org/10.1016/B978-0-12-800180-6.00003-7.

Watkins, D.J., Wellenius, G.A., Butler, R.A., Bartell, S.M., Fletcher, T., Kelsey, K.T., 2014. Associations between serum perfluoroalkyl acids and LINE-1 DNA methylation. Environ. Int. 63, 71–76. https://doi.org/10.1016/j.envint.2013.10.018.

Wen, L.L., Lin, L.Y., Su, T.C., Chen, P.C., Lin, C.Y., 2013. Association between serum perfluorinated chemicals and thyroid function in U.S. adults: the National Health and Nutrition Examination Survey 2007–2010. J. Clin. Endocrinol. Metab. 98 (9), E1456–E1464. https://doi.org/10.1210/jc.2013-1282.

Wilhelm, M., Kraft, M., Rauchfuss, K., Hölzer, J., 2008. Assessment and management of the first German case of a contamination with perfluorinated compounds (PFC) in the Region Sauerland, North Rhine-Westphalia. J. Toxicol. Environ. Health A. 71 (11–12), 725–733. https://doi.org/10.1080/15287390801985216.

Wilkinson, H.N., Hardman, M.J., 2017. The role of estrogen in cutaneous ageing and repair. Maturitas. 103, 60–64. https://doi.org/10.1016/j.maturitas.2017.06.026.

Willach, S., Brauch, H.J., Lange, F.T., 2016. Contribution of selected perfluoroalkyl and polyfluoroalkyl substances to the adsorbable organically bound fluorine in German rivers and in a highly contaminated groundwater. Chemosphere. 145, 342–350. https://doi.org/10.1016/j.chemosphere.2015.11.113.

Xu, Y., Jurkovic-Mlakar, S., Li, Y., Wahlberg, K., Scott, K., Pineda, D., et al., 2020. Association between serum concentrations of perfluoroalkyl substances (PFAS) and expression of serum microRNAs in a cohort highly exposed to PFAS from drinking water. Environ. Int. 136, 105446 https://doi.org/10.1016/j.envint.2019.105446.

Zhong, J., Liu, C., Chen, Y.J., et al., 2016. The association between S100A13 and HMGA1 in the modulation of thyroid cancer proliferation and invasion. J. Transl. Med. 14, 80. Published 2016 Mar 23. http://doi.org/10.1186/s12967-016-0824-x.

Zota, A.R., Geller, R.J., Romano, L.E., et al., 2018. Association between persistent endocrine-disrupting chemicals (PBDEs, OH-PBDEs, PCBs, and PFASs) and biomarkers of inflammation and cellular aging during pregnancy and postpartum. Environ. Int. 115, 9–20. https://doi.org/10.1016/j.envint.2018.02.044.